Effects of Temperature, Ti(III) Ion Concentration, and Current Density on Electrodeposition of Ti Films in LiF–LiCl Melt

Journal of The Electrochemical Society, 2022 **169** 092523

Effects of Temperature, Ti(III) Ion Concentration, and Current Density on Electrodeposition of Ti Films in LiF–LiCl Melt

Yutaro Norikawa,[1,*,z] Makoto Unoki,[1] Kouji Yasuda,[2,3,a,*] and Toshiyuki Nohira[1,*,z]

[1]*Institute of Advanced Energy, Kyoto University, Gokasho, Uji, Kyoto 611-0011, Japan*
[2]*Agency for Health, Safety and Environment, Kyoto University, Yoshida-Hommachi, Sakyo-ku, Kyoto 606-8501, Japan*
[3]*Graduate School of Energy Science, Kyoto University, Yoshida-Hommachi, Sakyo-ku, Kyoto 606-8501, Japan*

The effects of temperature, Ti(III) ion concentration, and current density on the electrodeposition of Ti films were investigated in the eutectic LiF–LiCl melt at 823–973 K. The Ti(III) ions were prepared by adding Li_2TiF_6 and Ti metal to the melt. The diffusion coefficients of Ti(III) were 1.4, 1.8, 2.3, and 3.2 × 10^{-5} m^2 s^{-1}, at 823, 873, 923, and 973 K, respectively. Galvanostatic electrolysis was conducted at 823–973 K. The surface roughness (S_a) of the Ti films decreases with decreasing temperature. Thus, the electrodeposition of Ti films was conducted at the lowest temperature of 823 K with various Li_3TiF_6 concentrations (0.55–7.1 mol%) and cathodic current densities (50–1200 mA cm^{-2}). The S_a was lower at higher Ti(III) ion concentrations and lower current densities. The smoothest Ti films with a S_a of 1.23 μm and a thickness of 10 μm were obtained at a cathodic current density of 50 mA cm^{-2} and Li_3TiF_6 concentration of 7.1 mol%.

 [DOI: 10.1149/1945-7111/ac91fe]

Manuscript submitted June 29, 2022; revised manuscript received September 8, 2022. Published September 27, 2022. *This paper is part of the JES Focus Issue on Nucleation and Growth: Measurements, Processes, and Materials.*

List of symbols

Symbol	Meaning	Unit
A	Electrode area	m^2
C_j	Concentration of species j	mol%
c_j	Concentration of species j	mol m^{-3}
D_j	Diffusion coefficient of species j	m^2 s^{-1}
D_j'	Pre-exponential constant	m^2 s^{-1}
F	Faraday constant	C mol^{-1}
I_{ap}	Anodic peak current	A
k	Boltzmann constant	J K^{-1}
n_j	Molar amount of species j	mol
R	Gas constant	J K^{-1} mol^{-1}
r	Ion radius	m
T	Temperature	K
v	Scan rate	V s^{-1}
W	Activation energy	J mol^{-1}
μ	Viscosity	Pa s

Titanium metal has excellent properties, such as a high specific strength, high corrosion resistance, and high biocompatibility, that are conducive to its use in aircraft components, chemical plants, medical components, etc. Furthermore, titanium is naturally abundant; however, its widespread use is hindered by its high smelting cost and poor workability. Titanium plating is an attractive technique to solve these problems because of its superior surface properties. Among titanium plating methods, electrolytic plating is a promising candidate as it delivers a higher deposition rate and shape flexibility. Previous reports have shown that metallic Ti can be electrodeposited only from high-temperature molten salts as electrolytes.[1–30] Nevertheless, pure titanium can only be electrodeposited from high-temperature molten salts.

In previous studies, chlorides,[1–15] fluorides,[16–20] and fluoride-chloride mixtures[5,13,15,21–30] have mainly been used as molten salt electrolytes. Generally, molten fluoride salts are preferable for the electrodeposition of compact and smooth titanium films. Robin et al. obtained comparatively compact and smooth films in LiF–NaF–KF melts at 873–923 K.[17–20] In the case of fluoride-chloride mixtures, several researchers have reported that Ti films with better morphology can be obtained from melts with sufficient fluoride concentrations. Takamura et al. reported that the morphology of deposits was improved by adding LiF to LiCl–KCl at 773 K.[5] Song et al. reported that Ti metal with fine crystal grains was obtained when KF was added to NaCl–KCl at 1073 K.[9] These reports indicate that fluoride ions have an important role for the electrodeposition of Ti film with smooth surface. Based on these reports, we focused on the electrodeposition of Ti in fluoride-chloride mixtures consisting of single cations with sufficient fluoride concentrations.[27–30] We have previously reported the electrochemical behavior of Ti(III) ions and the electrodeposition of Ti in molten KF–KCl (45:55 mol%, 923 K)[27–29] and LiF–LiCl (45:55 mol%, 923 K).[30] In our previous report, we optimized the current density and the Ti(III) ion concentration to obtain Ti films with smooth surface in molten KF–KCl at 923 K.[29] Further, we compared the electrochemical behaviors of Ti (III) in molten KF–KCl and LiF–LiCl at 923 K.[30] Although relatively smooth Ti films were obtained in these papers, the experiments were conducted only at 923 K and the effects of temperature were not investigated. Oki et al. reported that the surface morphology of deposited Ti changed with temperature and that Ti grains was lager at higher temperature.[23,24] They suggested that the smoother Ti films would be obtained at lower temperature. Therefore, it is worth investigating the effects of temperature, including low temperatures.

In this study, we selected a eutectic LiF–LiCl (LiF:LiCl = 30:70 mol%) with a low melting point of 774 K[31] to investigate the effects of temperature. The experiments were conducted at various temperatures of 823, 873, 923, and 973 K. We have explored the effects of temperature on the electrochemical behavior of Ti(III) ions and the smoothness of the Ti films. We conducted galvanostatic electrolysis at various Ti(III) ion concentrations and current densities to reveal their effects on the morphology and smoothness of the Ti films.

Experimental

Reagent-grade LiF (>99.0%; FUJIFILM Wako Pure Chemical Corp., Osaka, Japan, or Kojundo Chemical Laboratory Corp., Sakado, Japan) and LiCl (>99.0%; FUJIFILM Wako Pure Chemical Corp., Osaka, Japan, or Kojundo Chemical Laboratory Corp., Sakado, Japan) were dried under vacuum at 453 and 773 K

[a]Present address: Graduate School of Engineering, Kyoto University, Yoshida-hommachi, Sakyo-ku, Kyoto 606–8501, Japan.Present address: Graduate School of Engineering, Kyoto University, Yoshida-hommachi, Sakyo-ku, Kyoto 606–8501, Japan.
*Electrochemical Society Member.
[z]E-mail: norikawa.yutaro.6a@kyoto-u.ac.jp; nohira.toshiyuki.8r@kyoto-u.ac.jp

for more than 72 and 24 h, respectively. The salts were mixed in the eutectic composition (molar ratio of LiF:LiCl = 30:70, 300 g) and the mixture was loaded in a Ni crucible (Chiyoda Industry Manufacturing Plant Co. Ltd., Tokyo, Japan, outer diameter:98 mm, inner diameter: 96 mm, height: 102 mm) or a graphite crucible (Sanko Corp., Tokyo, Japan, outer diameter: 90 mm, inner diameter: 80 mm, and height: 120 mm). The crucible was placed at the bottom of a stainless-steel vessel in an airtight Kanthal container. Electrochemical measurements were conducted in a dry Ar atmosphere at 923 K in a glove box. After blank measurements in molten LiF–LiCl, Li_2TiF_6 and Ti metal (sponge or powder, >99%, Kojundo Chemical Laboratory Corp., Sakado, Japan) were added to the melt to prepare Ti(III) ions according to Eq. 1.

$$Ti + 3Li_2Ti(IV)F_6 + 6LiF \rightarrow 4Li_3Ti(III)F_6 \quad [1]$$

Here, added amount of Ti metal corresponds to approximately twice the amount necessary to generate Ti(III) ions from added Li_2TiF_6. Powdery Li_2TiF_6 was prepared by the same method as we reported previously.[30] Electrochemical measurements and galvanostatic electrolysis were performed via a three-electrode method with an electrochemical measurement system (Hokuto Denko Corp., HZ-7000, Tokyo, Japan). The working electrodes for electrochemical measurements were Mo flag (99.95%, Nilaco Corp., Tokyo, Japan, diameter: 3.0 mm, thickness: 0.1 mm) and Au flag (99.98%, Nilaco Corp., Tokyo, Japan, diameter: 3.0 mm, thickness: 0.1 mm). As shown in Fig. 1, the Au flag electrode consisted of a Au disk (diameter: 3.0 mm, thickness: 0.1 mm), to which a thin Au lead wire was welded (99.98%, Nilaco Corp., Tokyo, Japan, diameter: 0.1 mm). The structure of the Mo flag electrode was the same as the Au flag electrode. The substrate for galvanostatic electrolysis was the Ni plate (99.95%, Nilaco Corp., Tokyo, Japan, 10 mm × 10 mm, thickness: 0.1 mm). Ni was selected because of its good workability and proven experiences in electrodeposition of Ti films.[18,19,23,27,29] The Ni plates were rinsed with ethanol before the experiment. Ti rods (99.5%, Nilaco Corp., Tokyo, Japan, diameter: 3.0 mm) were used as the counter and reference electrodes. In the blank measurement, a Pt wire (Nilaco Corp., Tokyo, Japan, diameter: 1.0 mm, 99.98%) was used as the quasi-reference electrode. The potential of the reference electrodes was calibrated with respect to the dynamic Li^+/Li potential, as determined by cyclic voltammetry on a Mo electrode. The melt temperature was measured using a type K thermocouple. The salt adhering to the deposits was removed via an ultrasonic washing in distilled water for 10 min or by soaking in distilled water for 30 min and an aqueous $Al(NO_3)_3$ solution (1.0 mol dm^{-3}, obtained from FUJIFILM Wako Pure Chemical Corp., Osaka, Japan) for 10 min.

The surfaces and cross-sections of the samples were observed using a scanning electron microscope (SEM; Thermo Fisher Scientific Inc., Phenom Pro Generation 5, Waltham, MA). Before the observation of the cross-section, the samples were embedded in an acrylic resin and polished with emery papers and buffing compounds. The samples were then coated with Au using an ion-sputtering apparatus (Hitachi, Ltd., E-101, Tokyo, Japan) to impart conductivity. A small portion of the molten salt was sampled by the suction method using a borosilicate glass tube (outer diameter: 6 mm, inner diameter: 4 mm) and dissolved in aqueous HNO_3 solution (pH 1, Tama Chemical Corp., AA-100 grade, 68 wt%, Kawasaki, Japan). The solution was analyzed via inductively coupled plasma-atomic emission spectroscopy (ICP-AES; Hitachi, Ltd., SPECTRO BLUE, Tokyo, Japan) to determine the Ti ion concentration in the sampled molten salt.

Results and Discussion

Effect of temperature.— *Electrochemical measurement.*—The electrochemical reduction and oxidation of Ti(III) ions were investigated by cyclic voltammetry in the molten LiF–LiCl after adding 0.50 mol% of Li_2TiF_6 and 0.33 mol% of Ti sponge. Figure 2 shows the cyclic voltammograms in (a) the negative and (b) the positive potential regions at 823–973 K. In the negative potential

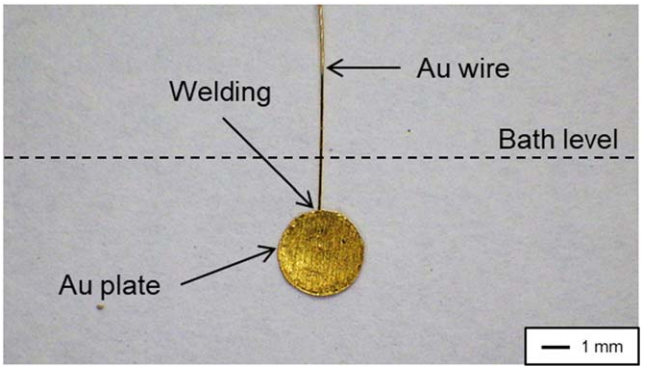

Figure 1. A photograph of a Au flag electrode. The electrode area is 0.157 cm^2.

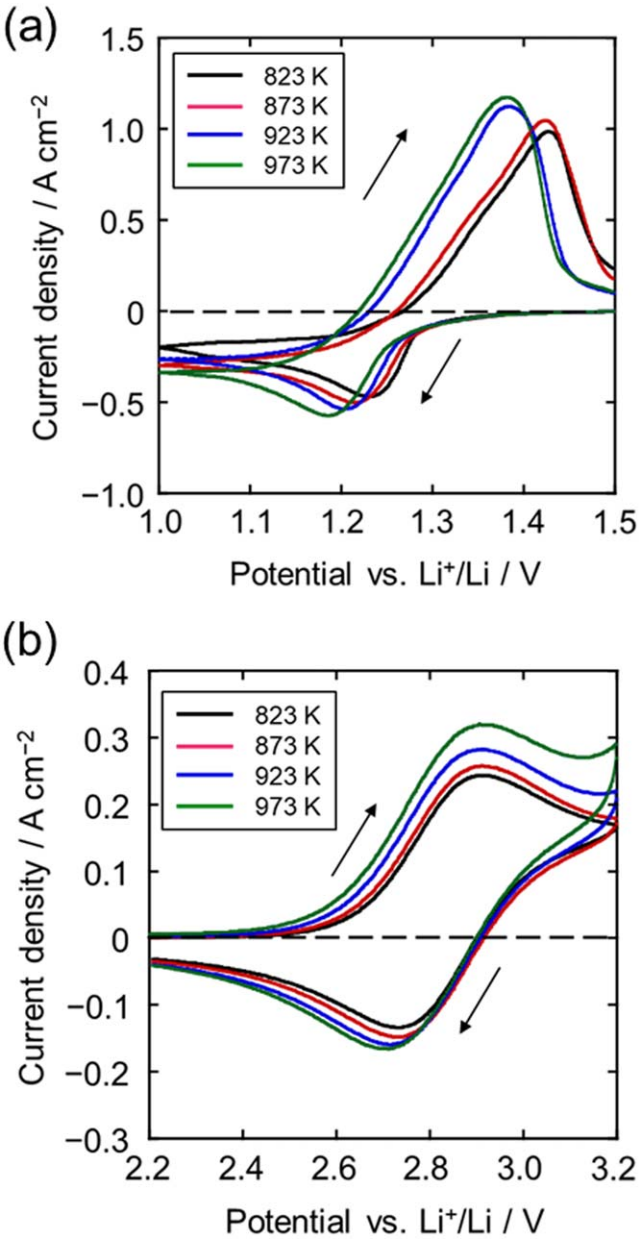

Figure 2. Cyclic voltammograms in LiF–LiCl melt after the addition of Li_2TiF_6 (0.50 mol%) and Ti sponge (0.33 mol%). (a) Negative potential region for a Mo flag electrode. (b) Positive potential region for a Au flag electrode.

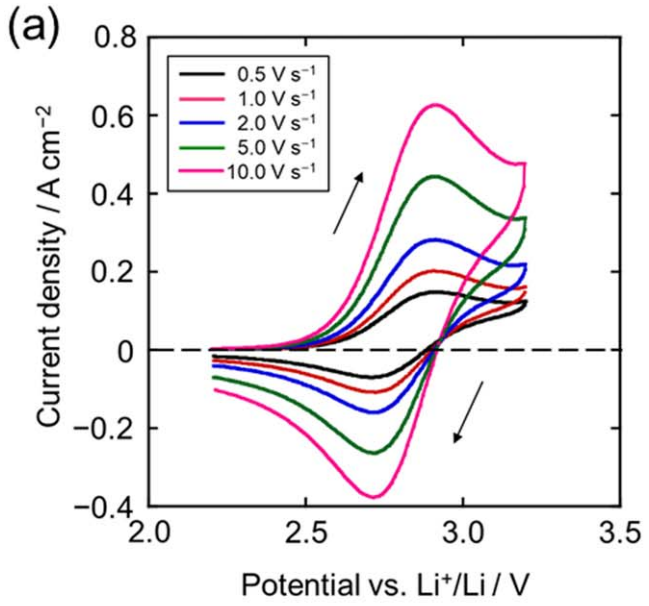

Figure 3. (a) Cyclic voltammograms for a Au flag electrode in molten LiF–LiCl after the addition of Li_2TiF_6 (0.50 mol%) and Ti sponge (0.33 mol%) at various scan rates at 923 K. (b) Dependence of anodic peak current density on scan rate at 823, 873, 923, and 973 K.

region, cathodic currents from 1.4 V vs Li^+/Li and peak potentials at 1.15–1.25 V are observed. In the positive potential region, redox currents are observed around 2.8 V. This behavior is similar to that of LiF–LiCl (45:55 mol%)–Li_3TiF_6 at 923 K.[30] Analogous to that case, the cathodic current around 1.2 V is due to Ti deposition from Ti(III) ions.

$$\mathrm{Ti(III)} + 3e^- \rightarrow \mathrm{Ti(0)} \quad [2]$$

The redox currents around 2.8 V were due to the redox reaction of Ti (IV)/Ti(III).

$$\mathrm{Ti(IV)} + e - \rightleftarrows \mathrm{Ti(III)} \quad [3]$$

The diffusion coefficient of the Ti(III) ions at each temperature was determined via cyclic voltammetry. Figure 3a shows the cyclic

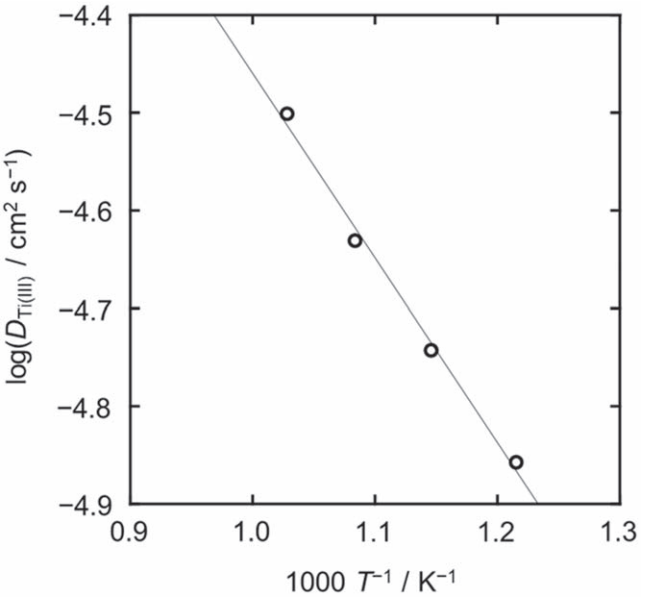

Figure 4. Arrhenius plot of diffusion coefficient of Ti(III) ions in molten LiF–LiCl after the addition of Li_2TiF_6 (0.50 mol%) and Ti sponge (0.33 mol%) at 823, 873, 923, and 973 K.

voltammograms obtained at various scan rates of 0.5 V s^{-1} to 10.0 V s^{-1} in the positive potential region at 923 K. Because the peak potentials of both the anodic and cathodic current peaks were constant at various scan rates, the redox reaction is a reversible process. In a reversible electrochemical reaction of soluble reactants and products, the anodic peak current (I_{ap}) is given by Eq. 4.[32]

$$I_{ap} = 0.446FAc_{Ti(III)}(D_{Ti(III)})(Fv/RT)^{1/2} \quad [4]$$

where A is the electrode area, $D_{Ti(III)}$ is the diffusion coefficient of Ti (III) ions, and v is the scan rate. The concentration of Ti(III) ions in the melt, $c_{Ti(III)}$, was calculated from the ICP-AES results and density of the LiF–LiCl melt. The density of the melt with a composition of LiF:LiCl = 30:70 mol% was estimated by extrapolating the reported data for the melts with LiF:LiCl = 37:63 and 25:75 mol% in the temperature range of 940–1260 K.[33] The estimated density values are 1.58, 1.56, 1.54, and 1.52 g cm^{-3} at 823, 873, 923, and 973 K, respectively. Figure 3b shows plots of the anodic peak current density against the square root of the scan rate in the range of 0.2–10 V s^{-1} at 823–973 K. The values of $D_{Ti(III)}$ in LiF–LiCl melt at 823, 873, 923, and 973 K are determined from the slopes of the plots to be 1.4, 1.8, 2.3, and 3.2 × 10^{-5} m^2 s^{-1}, respectively.

Figure 3 shows the Arrhenius plots created from the temperature dependence of $D_{Ti(III)}$. When the diffusion is dominated by an Arrhenius-type behavior, the diffusion coefficient varies according to Eq. 5.

$$D_{Ti(III)} = D'_{Ti(III)} \exp(-W/RT) \quad [5]$$

Here, $D'_{Ti(III)}$ is a constant, and W is the activation energy for diffusion. From the slope in Fig. 4, the activation energy is computed as 36.2 kJ mol^{-1}, and $D_{Ti(III)}$ is expressed as a function of the temperature.

$$D_{Ti(III)} = 2.69 \times 10^{-3} \times 10^{-1.89\times10^3/T} \quad [6]$$

Generally, the relationship between the diffusion coefficient and viscosity, μ, is given by the Stokes-Einstein equation in the diffusion of spherical particles in liquids with low Reynolds numbers[34]:

$$D = \frac{kT}{6\pi\tau\mu} \quad [7]$$

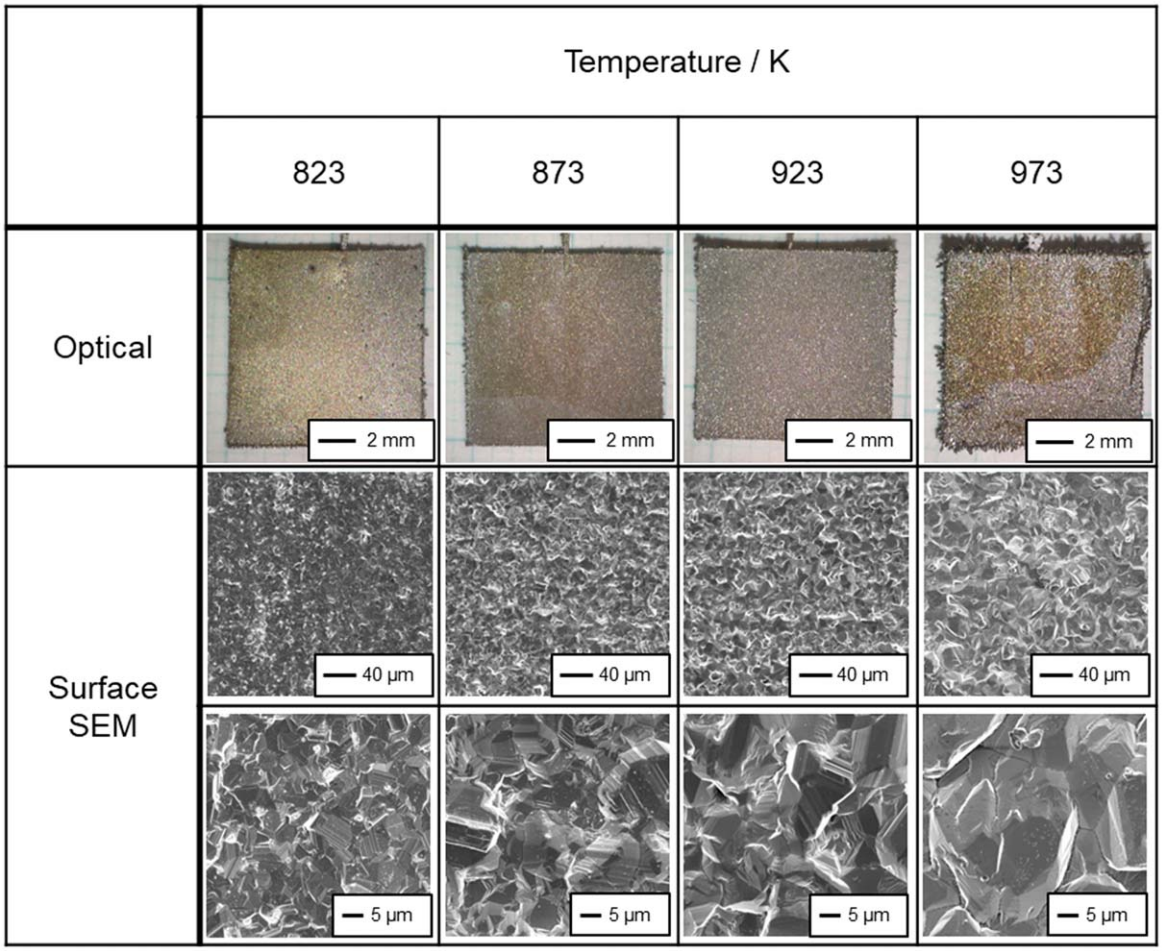

Figure 5. Optical and surface SEM images of the samples obtained by galvanostatic electrolysis for Ni plates in molten LiF–LiCl after the addition of Li_2TiF_6 (2.00 mol%) and Ti sponge (1.33 mol%) at 823, 873, 923, and 973 K. Cathodic current density: 100 mA cm^{-2}. Charge density: 60C cm^{-2}.

where k is the Boltzmann constant and r is the ion radius. From Eqs. 5 and 7, the following equation is obtained:

$$\ln(\mu/T) = \ln(k/6D'_{Ti(III)}r) + W/RT \quad [8]$$

From the reported temperature dependence of viscosity for both a single LiF melt and a single LiCl melt,[33] the calculated activation energies for LiF and LiCl are 26.0 and 29.3 kJ mol^{-1}, respectively. Compared with these, the value for the diffusion of Ti(III) ions was slightly larger. This result indicates that the diffusion of Ti(III) ions is strongly related to the viscosity of molten salts, according to the Stokes-Einstein equation.

Electrodeposition of Ti.—To investigate the effect of temperature on the smoothness of the Ti films, galvanostatic electrolysis was conducted at 823, 873, 923, and 973 K. Figure 5 shows the optical and surface SEM images of the samples obtained by galvanostatic electrolysis of Ni plates in molten LiF–LiCl after the addition of Li_2TiF_6 (2.00 mol%) and Ti sponge (1.33 mol%) at various temperatures. The cathodic current density and charge density were set at 100 mA cm^{-2} and 60C cm^{-2}, respectively. The Ti films obtained at all temperatures had a metallic luster, particularly, the sample at 823 K had a high brightness with a metallic luster. In addition, localized depositions near the substrate edges owing to the localized current distribution were more noticeable at higher temperatures. The grain sizes of the obtained Ti deposits increase with temperature, for example, several micrometers at 823 K and approximately 30 μm at 973 K.

The reason for the larger grain size at higher temperatures is discussed in the literature. Wei et al. reported the same tendency for NaCl–KCl–LiCl at 773–923 K with the addition of K_2TiF_6 and Ti metal powder.[23,24] The larger grain size was attributed to an increase in the diffusion coefficient of Ti ions and the diffusion rate of Ti atoms on the substrate surface. However, we deduced that the

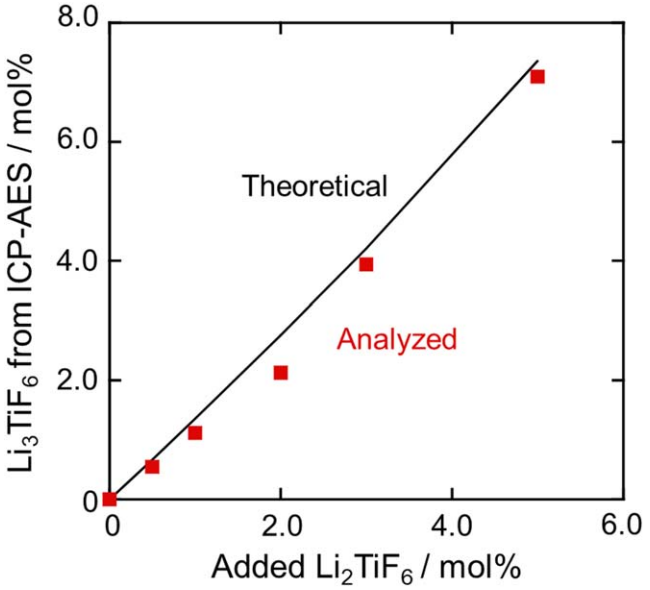

Figure 6. The concentration of Li_3TiF_6 determined by ICP-AES in molten LiF–LiCl after addition various amounts of Li_2TiF_6 (0–5.00 mol%) and Ti powder (0–3.33 mol%) at 823 K. Black line: Theoretical line. Red dots: Analyzed values.

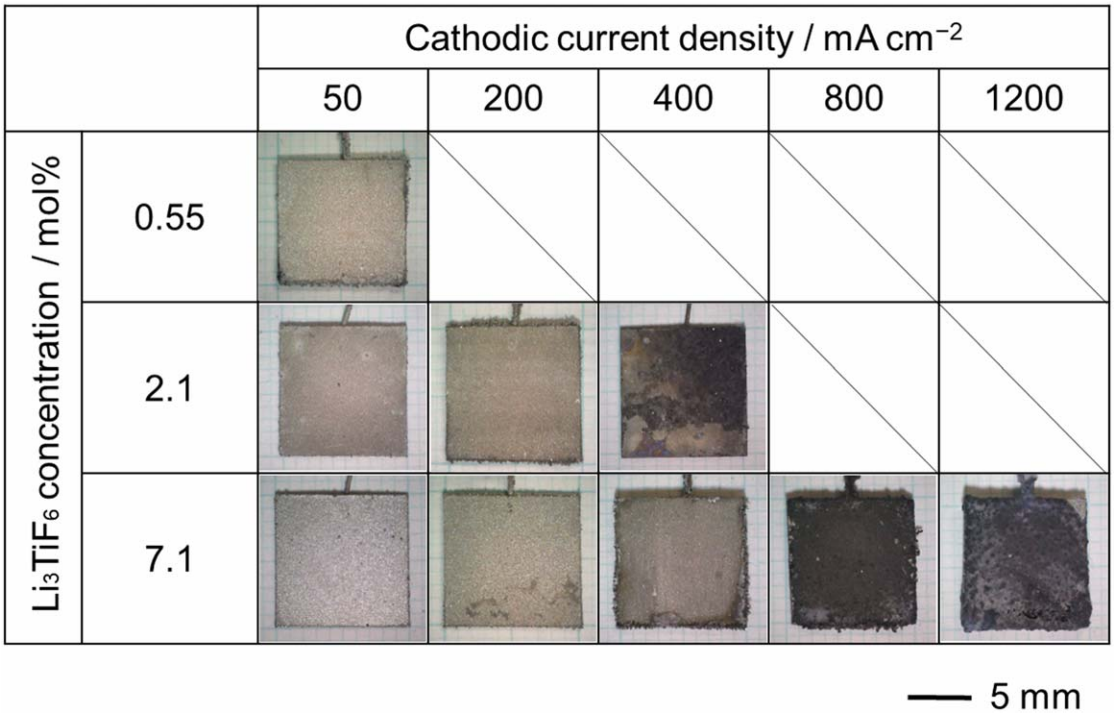

Figure 7. Optical images of the samples obtained by galvanostatic electrolysis for Ni plates at various Li_3TiF_6 concentrations (0.55, 2.1, 7.1 mol%) and cathodic current densities (50–1200 mA cm^{-2}) in molten LiF–LiCl at 823 K. Charge density: 60C cm^{-2}.

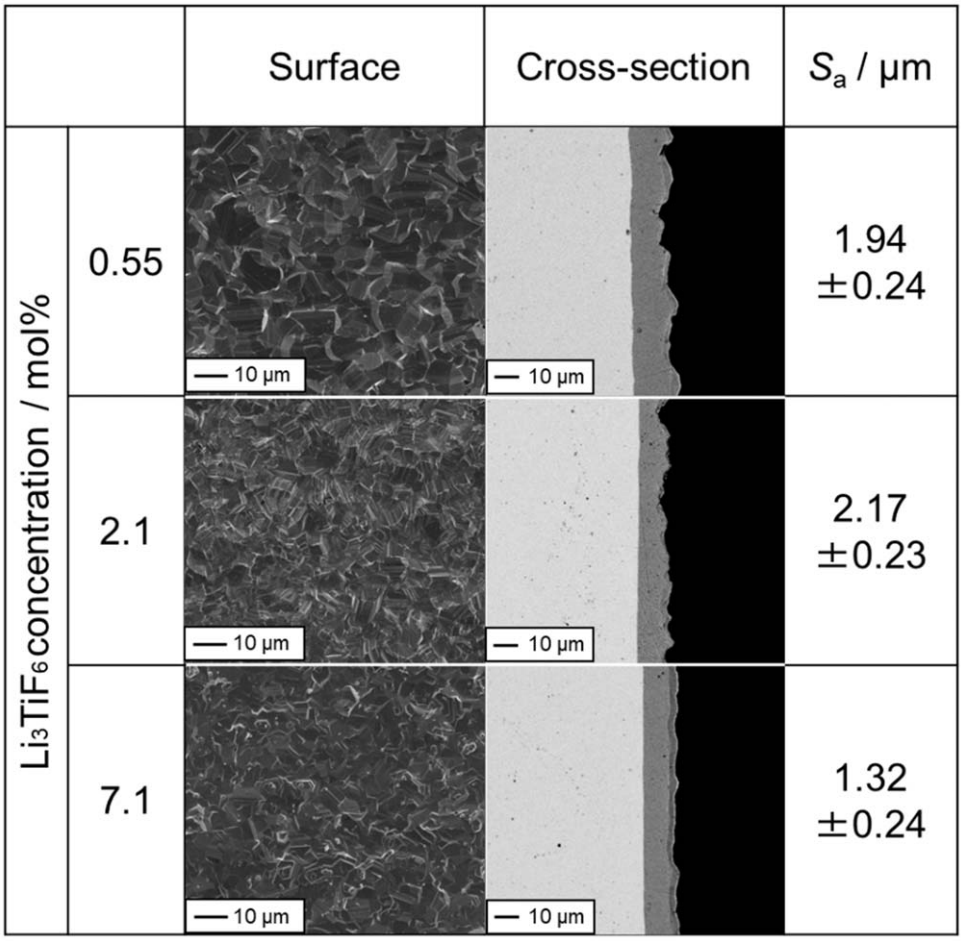

Figure 8. Surface and cross-sectional SEM images and surface roughness (S_a) of the samples obtained by galvanostatic electrolysis for plates at 50 mA cm^{-2} in LiF–LiCl–Li_3TiF_6 (0.55, 2.1, 7.1 mol%) at 823 K. Charge density: 60C cm^{-2}. Cathodic current density: 50 mA cm^{-2}. The S_a is average of 5 points.

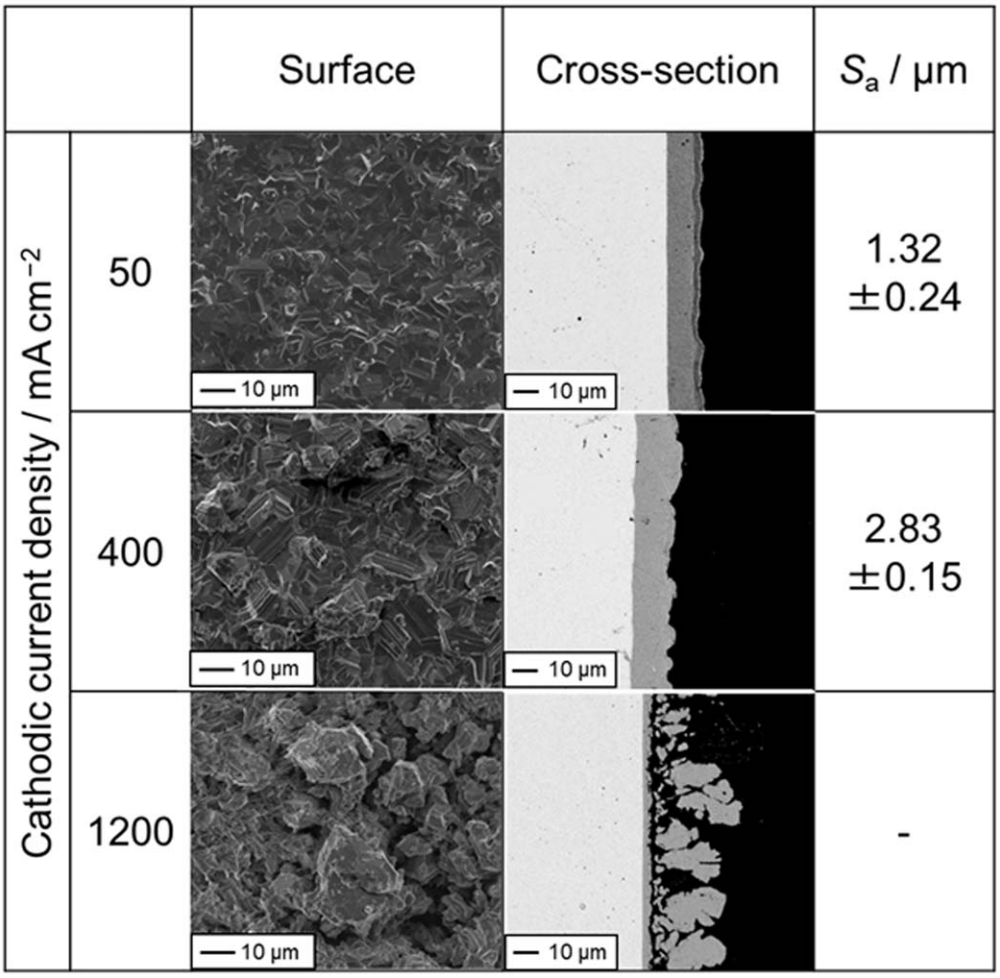

Figure 9. Surface and cross-sectional SEM images and surface roughness (S_a) of the samples obtained by galvanostatic electrolysis for Ni plates in LiF–LiCl–Li_3TiF_6 (7.1 mol%) at 823 K. Charge density: 60C cm^{-2}. Cathodic current density: 50, 400, 1200 mA cm^{-2}. The S_a is the average of 5 points.

Table I. Surface roughness of the samples obtained at various temperatures. Electrolysis conditions are the same as Fig. 4. The value is the average of 5 points. Narrow range: 401 × 401 μm (area), 80 μm (cut-off length). Wide range: 1.2 × 1.2 mm (area), 240 μm (cut-off length).

	Measurement range	Temperature K^{-1}			
		823	873	923	973
Surface roughness (S_a)/μm	Narrow	1.12 ±0.16	3.61 ±0.29	3.78 ±0.21	3.59 ±0.35
	Wide	2.05 ±0.22	4.58 ±0.31	5.00 ±0.65	5.71 ±0.92

recrystallization and grain growth of Ti were reasonable. Okazaki and Conrad reported the recrystallization and grain growth of Ti by vacuum annealing at 773–1073 K.[35] After annealing for 2 h, the grain size increased from the original size of 1 μm to 2–50 μm depending on the temperature. The grain sizes at 773 and 973 K were approximately 2 and 20 μm, respectively. Considering the reported results, the grain sizes of several micrometers at 823 K and 30 μm at 973 K obtained by electrodeposition in the present study are reasonably explained by a temperature-dependent grain growth.

Table I lists the surface roughness (S_a) values of the samples shown in Fig. 4. The measurements were carried out in two ranges, narrow range: 401 × 401 μm (area), 80 μm (cut-off length) and wide range: 1.2 × 1.2 mm (area), 240 μm (cut-off length). The value of S_a increased with an increase in the bath temperature. It should be noted that S_a at 823 K is especially small and almost the same with that of the original Ni substrate (S_a = 1.2 μm for narrow range analysis). Because Ti films with smooth surfaces were successfully obtained at the lowest temperature of 823 K, the effect of the Ti(III) ion concentration and cathodic current density was investigated at 823 K.

Effect of Ti(III) ion concentration and current density.—*Determination of Ti(III) ion concentration.*—Before electrodeposition, the concentration of Li_3TiF_6 was investigated via ICP-AES measurements. Figure 6 shows the plots of the concentrations of Li_3TiF_6 against the added amounts of Li_2TiF_6. The molar amount of formed Li_3TiF_6 and the corresponding consumed LiF according to Eq. 1 was obtained from the ICP analytical result of weight concentration for Ti. Then, the molar fraction of Li_3TiF_6, $C_{Li_3TiF_6}$,was calculated by the following equation:

$$C_{Li_3TiF_6} = n_{Li_3TiF_6}/(n_{LiF} + n_{LiCl} + n_{Li_3TiF_6}) \times 100 \quad [9]$$

Here, $n_{Li_3TiF_6}$, n_{LiF}, and n_{LiCl} indicate the molar amounts of Li_3TiF_6, LiF, and LiCl in the molten salt, respectively. The theoretical concentration of Li_3TiF_6 is not simply four-thirds of the added amount of Li_2TiF_6 because of the consumption of LiF according to Eq. 1. Therefore, the theoretical value is not completely linear with the added amounts of Li_2TiF_6. As shown in Fig. 6, the analyzed values are close to the theoretical values. The concentration of Li_3TiF_6 at the addition of 5.0 mol% Li_2TiF_6 was 7.1 mol%, and this value has not yet reached saturation.

Electrodeposition of Ti films.—To investigate the effects of the Ti (III) ion concentration and cathodic current density on the morphology and smoothness of Ti electrodeposits, galvanostatic electrolysis was conducted at various Li_3TiF_6 concentrations (0.55, 2.1, 7.1 mol%) and current densities (50–1200 mA cm^{-2}). The electric charge density was fixed at 60C cm^{-2} for all electrolysis processes. Figure 7 shows the optical images of the electrodeposited samples after washing the adherent salts. Compact and highly adherent Ti films were obtained at 50 mA cm^{-2} for all Li_3TiF_6 concentrations. As the concentration increased, compact and adherent Ti films were obtained even at higher current densities, up to 200 mA cm^{-2} at 2.1 mol% Li_2TiF_6 and up to 400 mA cm^{-2} at 7.1 mol%. However, the morphology of the deposits changed to powder-like as the current density further increased.

Figure 8 shows a comparison of the surface/cross-sectional SEM images and surface roughness (S_a) at the same current density (50 mA cm^{-2}) at various Li_3TiF_6 concentrations. The surface roughness measurements were carried out in a wide range:1.2 × 1.2 mm (area) and 240 μm (cut-off length). The formation of compact and adherent Ti films was also confirmed by SEM images. The film thickness was 10–15 μm, which is smaller than the theoretical value of 22 μm due to localized deposition on a lead wire and near edges of substrate. The differences in thickness on the conditions might be caused by the same reason. In addition, an inter-diffusion layer with the thickness less than 1 μm was observed between Ti film and Ni substrate. The smoothness of the deposits improved with increasing Li_3TiF_6 concentration. The smallest S_a (1.32 μm), which indicates the smoothest surface, was obtained at 7.1 mol% of Li_3TiF_6. Notably, this value is almost the same as that of the Ni substrate measured by the same method (S_a = 1.23 μm).

Figure 9 shows the surface/cross-sectional SEM images and surface roughness (S_a) at the same Li_3TiF_6 concentration (7.1 mol%) at various current densities. At 400 mA cm^{-2}, the compactness and adhesion were almost the same as those at 50 mA cm^{-2}. However, the surface roughness increased and nodule electrodeposits were partially observed. At a very high current density of 1200 mA cm^{-2}, the morphology of the electrodeposits was powder-like and the adhesion was quite low.

Conclusions

The effects of temperature, Ti(III) ion concentration, and cathodic current density on the electrodeposition of Ti films were investigated in the eutectic LiF–LiCl melt at 823–973 K. Ti(III) ions were generated by the addition of Li_2TiF_6 and Ti metal to the melt. The diffusion coefficient of Ti(III) ions was determined as a function of temperature as $D_{Ti(III)} = 2.69 \times 10^{-3} \times 10^{-1.89\times10^3/T}$ (m^2 s^{-1}). SEM observations and surface roughness (S_a) measurements revealed that smoother Ti films were electrodeposited at lower temperatures. This can be explained by the temperature dependence of Ti grain growth. At higher Ti(III) concentrations and lower cathodic current densities, smoother Ti films are electrodeposited. The smoothest Ti films with a surface roughness of 1.23 μm and thickness of 10 μm were obtained at 50 mA cm^{-2}, 7.1 mol% of Li_3TiF_6, and 823 K.

Acknowledgments

Part of this study was conducted in collaboration with Sumitomo Electric Industries Ltd. Part of this work was supported by JSPS Fellows Grant Number 19J15015.

ORCID

Yutaro Norikawa https://orcid.org/0000-0002-0861-5443
Kouji Yasuda https://orcid.org/0000-0001-5656-5359
Toshiyuki Nohira https://orcid.org/0000-0002-4053-554X

References

1. M. B. Alpert, F. J. Schultz, and W. F. Sullivan, *J. Electrochem. Soc.*, **104**, 555 (1957).
2. B. J. Fortin, J. G. Wurm, L. Gravel, and R. J. A. Potvin, *J. Electrochem. Soc.*, **106**, 428 (1959).
3. A. Menzies, D. L. Hill, G. J. Hills, L. Young, and J. O. M. Bockris, *J. Electroanal. Chem.*, **1**, 161 (1959).
4. G. M. Haarberg, W. Rolland, A. Sterten, and J. Thonstad, *J. Appl. Electrochem.*, **23**, 217 (1993).
5. H. Takamura, I. Ohno, and H. Numata, *J. Jpn. Inst. Metals*, **60**, 388 (1996).
6. X. Ning, H. Asheim, H. Ren, S. Jiao, and H. Zhu, *Metall. Mater. Trans. B*, **42**, 1181 (2011).
7. T. Yuan, Q.-g Weng, Z. Zhou, J. Li, and Y.-h He, *Adv. Mater. Res.*, **284–286**, 1477 (2011).
8. M. H. Kang, J. Song, H. Zhu, and S. Jiao, *Metall. Mater. Trans. B*, **46**, 162 (2015).
9. J. Song, Q. Wang, M. Kang, and S. Jiao, *Int. J. Electrochem. Sci.*, **10**, 919 (2015).
10. S. Wang, C. Wan, X. Liu, and L. Li, *Metall. Mater. Trans. E*, **2**, 250 (2015).
11. S. Tokumoto, E. Tanaka, and K. Ogisu, *JOM*, **27**, 18 (1975).
12. J. G. Gussone and J. M. Hausmann, *J. Appl. Electrochem.*, **41**, 657 (2011).
13. J. Song, Q. Wang, X. Zhu, J. Hou, S. Jiao, and H. Zhu, *Mater. Trans.*, **55**, 1299 (2014).
14. A. Kishimoto, Y. Yamada, K. Funatsu, and T. Uda, *Adv. Eng. Mater.*, **22**, 1900747 (2019).
15. K. Kumamoto, A. Kishimoto, and T. Uda, *Mater. Trans.*, **61**, 1651 (2020).
16. K. Matiašovsky, Ž. Lubyovà, and V. Daněk, *Electrodepos. Surface Treat.*, **1**, 43 (1972).
17. J. De Lepinay, J. Bouteillon, S. Traore, D. Renaud, and M. J. Barbier, *J. Appl. Electrochem.*, **17**, 294 (1987).
18. A. Robin, J. De Lepinay, and M. J. Barbier, *J. Electroanal. Chem.*, **230**, 125 (1987).
19. A. Robin, *Mater. Lett.*, **34**, 196 (1998).
20. A. Robin and R. B. Ribeiro, *J. Appl. Electrochem.*, **30**, 239 (2000).
21. M. E. Sibert and M. A. Steinberg, *J. Electrochem. Soc.*, **102**, 641 (1955).
22. J. G. Wurm, L. Gravel, and R. J. A. Potvin, *J. Electrochem. Soc.*, **104**, 301 (1957).
23. D. Wei, T. Tada, and T. Oki, *ISIJ Int.*, **33**, 1016 (1993).
24. D. Wei, M. Okido, and T. Oki, *J. Appl. Electrochem.*, **24**, 923 (1994).
25. J. H. von Barner, P. Noye, A. Barhoun, and F. Lantelme, *J. Electrochem. Soc.*, **152**, C20 (2005).
26. V. V. Malyshev and D. B. Shakhnin, *Mater. Sci.*, **50**, 80 (2014).
27. Y. Norikawa, K. Yasuda, and T. Nohira, *Mater. Trans.*, **58**, 390 (2017).
28. Y. Norikawa, K. Yasuda, and T. Nohira, *Electrochemistry*, **86**, 99 (2018).
29. Y. Norikawa, K. Yasuda, and T. Nohira, *J. Electrochem. Soc.*, **166**, D755 (2019).
30. Y. Norikawa, K. Yasuda, and T. Nohira, *J. Electrochem. Soc.*, **167**, 082502 (2020).
31. J. Sangster and A. D. Pelton, *J. Phys. Chem. Ref. Data*, **16**, 509 (1987).
32. R. S. Nicholson and I. Shain, *Anal. Chem.*, **36**, 706 (1964).
33. G. J. Janz, *J. Phys. Chem. Ref, Data*, **17**, Suppl. 2, 1 (1988).
34. A. Einstein, *Investigations on the Theory of the Brownian Movement* (Dover Publications Inc, New York, NY) (1956).
35. K. Okazaki and H. Conrad, *Metall. Trans.*, **3**, 2411 (1972).